Optical properties of TiO2:Ag composites

Krzysztof Skorupski[a]

[a]Wroclaw University of Technology, Chair of Electronics and Photonics Metrology, Boleslawa Prusa 53/55, 50-317 Wroclaw, Poland

ABSTRACT

The main goal of our research was to investigate the optical properties of nanocomposites, created by combining titanium dioxide with noble metals. Our research was focused on silver Ag, which reveals strong plasmonic effects in the visible spectrum, and rutile TiO_2 - a commonly used semiconductor material that does not present any significant optical properties in the mentioned range of electromagnetic waves. Our results show that when coating is considered (i.e. the TiO_2 particle is covered by an additional Ag layer) the position of the extinction peak can be manipulated and shifted towards lower wavelengths. However, when the main TiO_2 particle is surrounded by small Ag spheres, such extinction peak occurs at a fixed wavelength only and cannot be adjusted.

Keywords: rutile, silver, nanocomposites, light scattering

1. INTRODUCTION

Titanium dioxide is a commonly used semiconductor material. It is non-toxic, non-expensive and broadly available.[1] It can be used in various gas sensors or in specific photovoltaic applications.[1,2] Its well-recognized antibacterial activity is an additional advantage.[3,4] However, the greatest limitation is the fact that no interesting optical properties are present in the visible spectrum, i.e. from $\lambda \approx 400nm$ to $\lambda \approx 800nm$. Recent study suggest that this disadvantage can be fixed by implementing an additional volume of noble metals on its surface, for example in a form of silver Ag or gold Au nanoparticles.[2] In our work we are interested in the extinction efficiency Q_{ext} of such composites, which is related to the extinction cross section C_{ext} in the following manner:

$$Q_{ext} = \frac{C_{ext}}{\pi R_v^2}, Q_{sca} = \frac{C_{sca}}{\pi R_v^2}, Q_{abs} = \frac{C_{abs}}{\pi R_v^2}, \tag{1a}$$

$$Q_{ext} = Q_{sca} + Q_{abs}, \tag{1b}$$

where R_v is the radius of a volume-equivalent sphere, Q_{sca} denotes the scattering efficiency and Q_{abs} is the absorption efficiency.

2. GENERATED COMPOSITES

The modeling process is the first step to understand the physics behind various phenomena.[5] In our work two different types of composites are studied. The first of them consists of a main particle with the radius R_m and a solid layer. To achieve the chosen volume ratio, the amount of the second material V_l must be adjusted accordingly. Therefore, the total radius of the composite R_c increases gradually while the volume of the main particle V_m remains constant, what is presented in Fig. 1 and described by the following equations:

$$ratio = V_l/(V_m + V_l), \tag{2a}$$

$$R_c = (1 - ratio)^{-1/3} \cdot R_m. \tag{2b}$$

The second composite type also consists of a main particle. However, this time it is surrounded by small, monodisperse spheres with the radius R_s instead of a solid layer. In our model particles do not tend to overlap. The volume of the second material V_s is proportional to the number of covering spheres N_s, which is defined as:

$$N_s \approx (ratio/\,(1 - ratio))\,(R_m/R_s)^3\,. \tag{3}$$

E-mail: krzysztof.skorupski@pwr.wroc.pl

Metamaterials IX, edited by Allan D. Boardman, Nigel P. Johnson, Kevin F. MacDonald, Ekmel Özbay, Proc. of SPIE Vol. 9125, 91251J · © 2014 SPIE · CCC code: 0277-786X/14/$18 · doi: 10.1117/12.2052262

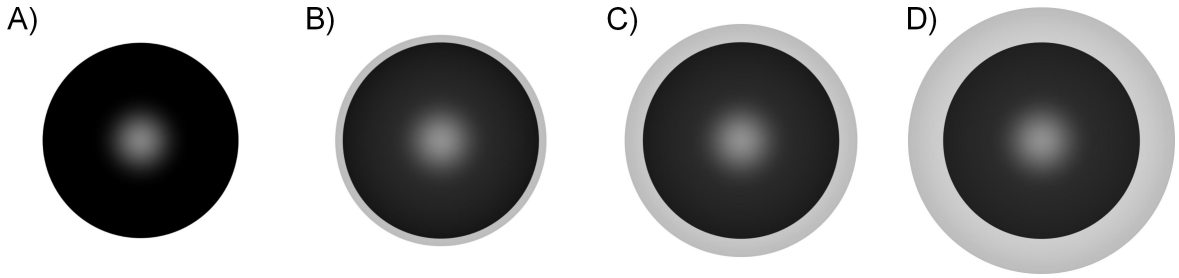

Figure 1: The picture presents the main TiO_2 particle surrounded by an additional silver Ag or gold Au layer. The volume ratio is $ratio = 0\%$, $ratio = 10\%$, $ratio = 30\%$ and $ratio = 50\%$ respectively. The radius of the main particle R_m is always constant.

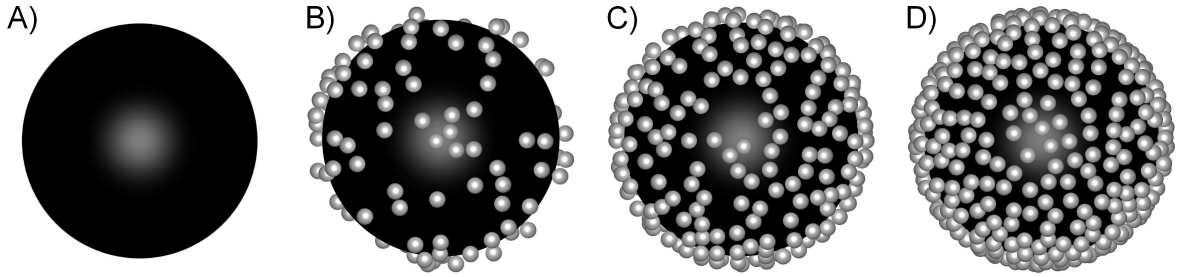

Figure 2: The picture presents the main TiO_2 particle surrounded by silver Ag or gold Au spheres. Their quantity is $N_s = 0$, $N_s = 124$, $N_s = 260$ and $N_s = 407$,respectively. The radius of the main particle R_m is always constant.

In our approach, to set the exact volume of the second material V_s, the number of spheres N_s is lowered to the first integer value and their size (defined by R_s) is adjusted accordingly. Because the number of surrounding spheres N_s is significant, such changes are barely visible. Note, that the maximum volume of the composite V_c is limited, what is associated with the estimated value of R_s. The second composite type is presented in Fig. 2. In both cases the radius of the main particle was $R_m = 36nm$ and the radius of surrounding spheres was assumed to be $R_s \approx 2.5nm$. The mentioned morphological parameters were based on the paper by Hari et al.[2] The refractive index of titanium dioxide m_{TiO_2} was adapted from the paper by Landmann et al. (see Fig. 4)[1] and the refractive index of silver m_{Ag} was based on the work by Palik (see Fig. 3).[6,7] Note, that our structures are theoretical - the polydispersity is neglected and particles are modeled as perfect spheres. The morphological parameters are not considered universal as well (in other papers they can differ significantly).[3] Whereas the first composite type is purely theoretical, the second one can be generated under laboratory conditions. A sample procedure is presented in the work by Hari et al.[2] and by Martinez et al.[3]

3. LIGHT SCATTERING SIMULATIONS

Light scattering measurements, or analysis of TEM (Transmission Electron Microscopy) images, are a common technique to characterize the morphological parameters of different structures.[8–12] In our work we used two alternative codes which are capable of simulating the amount of the light scattered by assemblies of spheres positioned in point contact. The first of them was GMM (Generalized Multiparticle Mie-Solution) code by Y. Xu[13] and the second one was a superposition T-Matrix code created by D. Mackowski.[14] When a single sphere is considered, both programs give the same results, which are based on the classic Mie solution. When an assembly of spheres is considered, the results may slightly differ. To check the possible error between two methods a sample structure, composed of a single rutile TiO_2 particle and $N_c = 15$ surrounding silver Ag spheres, was generated. The maximum relative error between both approaches was $E_{rel,\lambda=370nm} \approx 8.56\%$ and occurred at the wavelength of $\lambda = 370nm$. However, for each other λ it was much lower and the averaged value (arithmetic mean), for the spectrum from $\lambda = 200nm$ to $\lambda = 1600nm$, was ca. $E_{rel} \approx 0.48\%$. We conclude that this

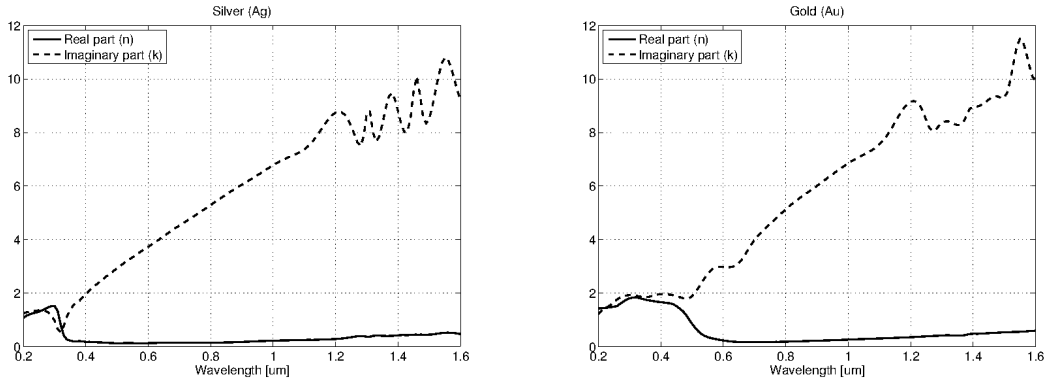

Figure 3: In the picture the complex refractive indices m for gold Au and silver Ag are presented. Their values are based on the work by E. Palik.[6,7]

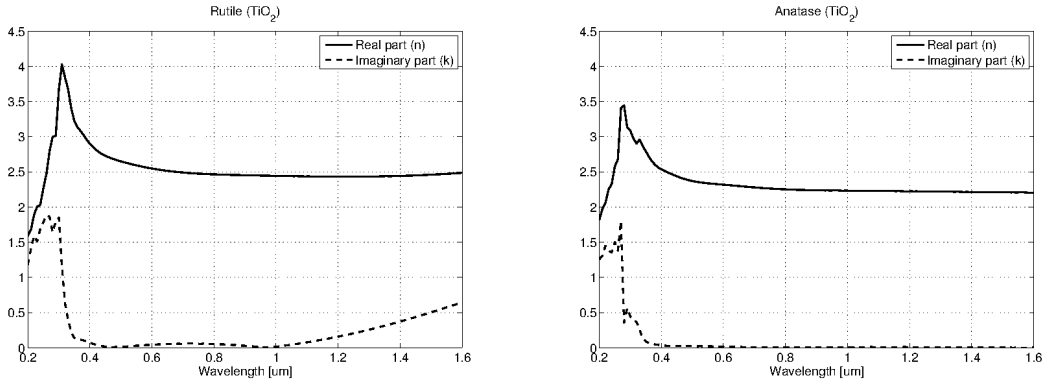

Figure 4: In the picture the complex refractive indices m for rutile and anatase are presented. Their values are based on the work by Landmann et al.[1] The last TiO_2 state - brookite, was not investigated in our work.

difference is small enough to use both techniques interchangeably. The main problem with our simulations was the exceptional computation time. Calculations were performed on a standard PC with 8GB RAM and AMD Athlon II X4 640 (3.00 GHz) processor. For $TiO_2(rutile) : Ag$ composites with $N_s = 407$ surrounding spheres at the wavelength of ca. $\lambda \approx 370nm$ our simulations took ca. 13.5 hours. The maximum calculation time was observed for $TiO_2(anatase) : Ag$ composites characterized by the same number of surrounding particles, i.e. $N_s = 407$, at the wavelength of ca. $\lambda \approx 400nm$, which turned out to be ca. 23.5 hours (the results for $TiO_2(rutile) : Ag$ composites immersed in water are not compared because the simulations were performed on a different machine). Note, that in our study the wavelength step is $\Delta\lambda = 10nm$ and all composites were investigated within the electromagnetic spectrum from $\lambda = 200nm$ to $\lambda = 1400nm$ minimum (in spite of the fact that in some figures, when no interesting optical effects were observed, this spectrum was limited).

3.1 Coating

In the first step of our study, to have a better overview of the investigated problem, the extinction efficiency Q_{ext} for different types of particles was calculated and the results are presented in Fig. 5. Next, a single rutile TiO_2 particle was covered by an additional silver Ag layer with variable thickness. The volume ratio varied from $ratio = 0\%$ to $ratio = 70\%$. The light scattering simulations were performed with the GMM algorithm[13] and the resulting diagrams are presented in Fig. 6. Providing that the silver Ag layer is relatively small, e.g. $R_c - R_m = 1.3nm$, only minor aberrations occur in the non-visible spectrum from $\lambda = 1000nm$ to $\lambda = 2000nm$. However, when the surrounding layer is thicker - the second extinction peak appears. Its position can be easily controlled by the volume of the second material V_l. For larger values, i.e. greater than $R_c - R_m > 6.5nm$, the

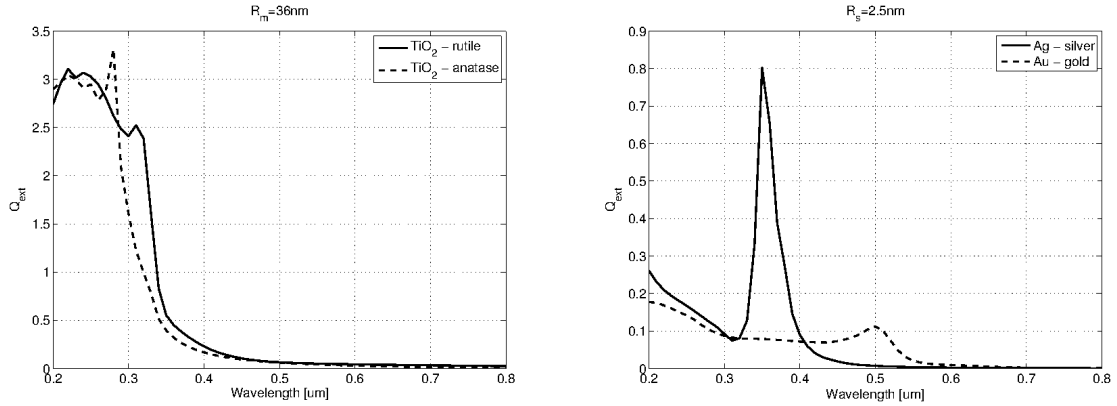

Figure 5: Extinction efficiency Q_{ext} as a function of the incident wavelength λ. Two particle types, i.e. the main particle and a surrounding particle, are presented.

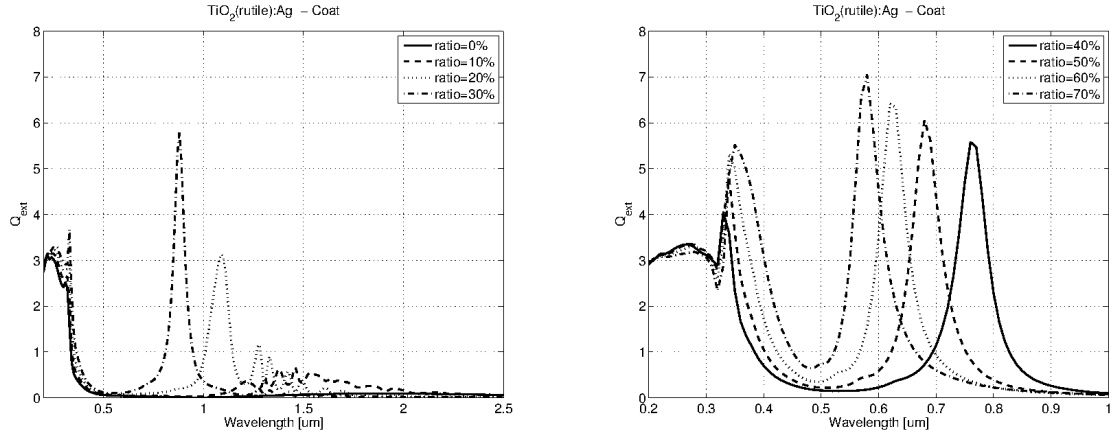

Figure 6: Extinction efficiency Q_{ext} as a function of the incident wavelength λ for $TiO_2(rutile) : Ag$ composites. The main TiO_2 particle is covered by an additional Ag layer with variable thickness.

peak is shifted to the visible spectrum. The main advantage of this approach is the simulation time. However, this structure is more theoretical than the second composite type.

3.2 Surrounding particles

Next, a single rutile TiO_2 particle was surrounded by silver Ag spheres with the radius $R_s = 2.5nm$. The light scattering results, presented in Fig. 7, show that silver Ag particles are responsible for the extinction peak that occurs at the wavelength of ca. $\lambda \approx 350nm$. Its location cannot be shifted and its magnitude depends on the number of surrounding silver Ag spheres. No spectral effects were observed at the wavelength of $\lambda = 600nm$ and above - in this regime, the presence of silver Ag particles has negligible impact on the results. However, this effect might be associated with the amount of the second material V_s, which is limited by the volume ratio of 12%. It was difficult to place more spheres on the surface of the main particle at random. In Fig. 8 a comparison of the extinction efficiency Q_{ext} between both composite types is presented. The dotted line defines the volume of the silver Ag layer which is equivalent to $N_c = 407$ surrounding particles with the radius $R_s \approx 2.5nm$. The dashed line is associated with the silver Ag layer characterized by the thickness $R_c - R_m = 2R_s$. The results prove that these two approaches cannot be used interchangeably. When surrounding spheres are considered, the position of the extinction peak is closely related to the optical response of a single silver A_g particle (see Fig. 5). By the contrary, when a solid silver Ag layer is studied, the optical response of the composite changes significantly. Providing that the volume ratio is as large as 32% the first extinction peak is visible below the wavelength of

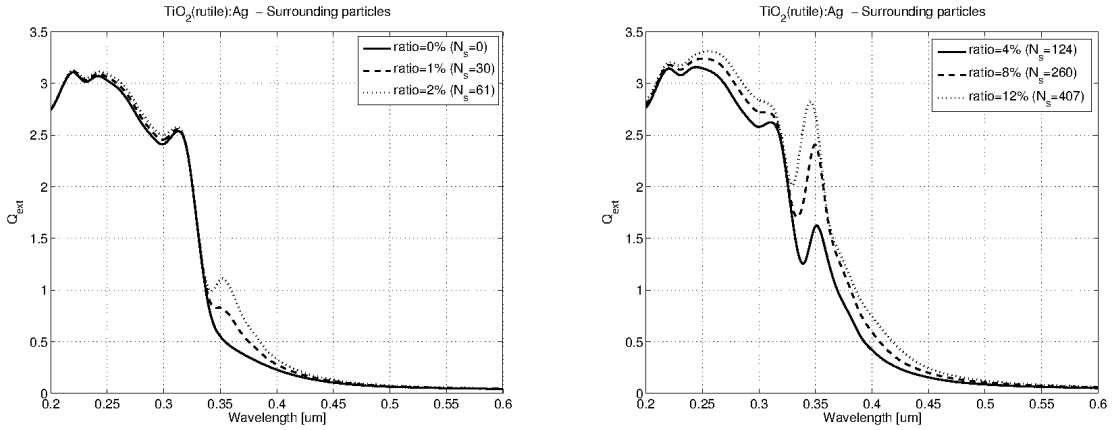

Figure 7: Extinction efficiency Q_{ext} as a function of the incident wavelength λ for $TiO_2(rutile) : Ag$ composites. The main TiO_2 particle is surrounded by Ag spheres, which are responsible for the extinction peak that occurs at the wavelength of ca. $\lambda \approx 350nm$.

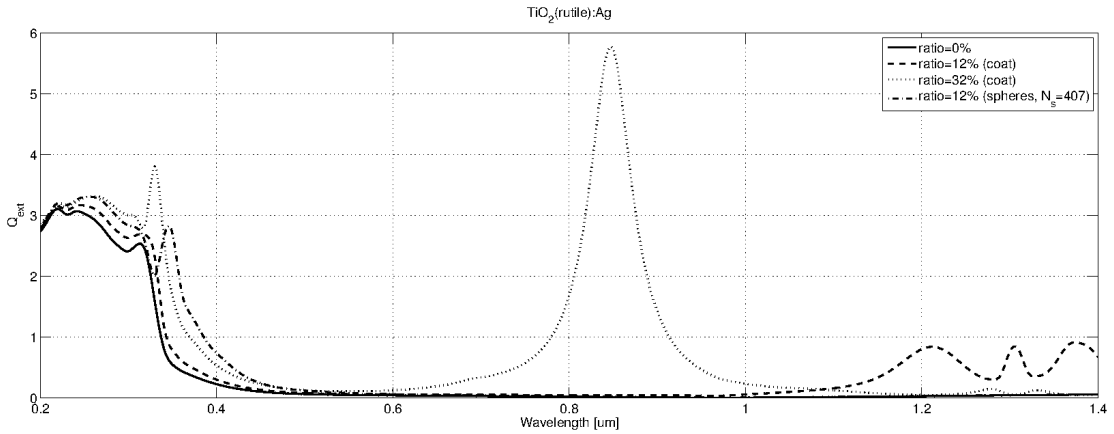

Figure 8: Extinction efficiency Q_{ext} as a function of the incident wavelength λ for $TiO_2(rutile) : Ag$ composites. The comparison between two composite types is presented.

$\lambda < 350nm$ and the second one occurs at ca. $\lambda \approx 840nm$. When the volume ratio is 12% no significant optical effects are observed.

3.3 Additional simulations

In our work we were also interested in other composite types, i.e. $TiO_2(rutile) : Au$, $TiO_2(anatase) : Ag$, $TiO_2(anatase) : Ag$ and $TiO_2(rutile) : Ag$ positioned in water instead of vacuum. The results are presented in Fig. 9, Fig. 10, Fig. 11 and Fig. 12. Their behavior is similar to our former study and no surprising spectral effects were observed. When small gold Au spheres were considered, the extinction peak at ca. $\lambda \approx 350nm$ was not visible. However, an increased value of the extinction efficiency Q_{ext} was observed at the wavelength of ca. $\lambda \approx 500nm$. This phenomenon is associated with the response of small, surrounding gold Au spheres (see Fig. 5).

4. CONCLUSIONS

In our work we investigated the optical properties of nanocomposites, created by combining titanium dioxide with noble metals. Our research was mostly focused on silver Ag and rutile TiO_2 particles. Our results show that Ag particles are responsible for the extinction peak that occurs at the wavelength of ca. $\lambda \approx 350nm$.

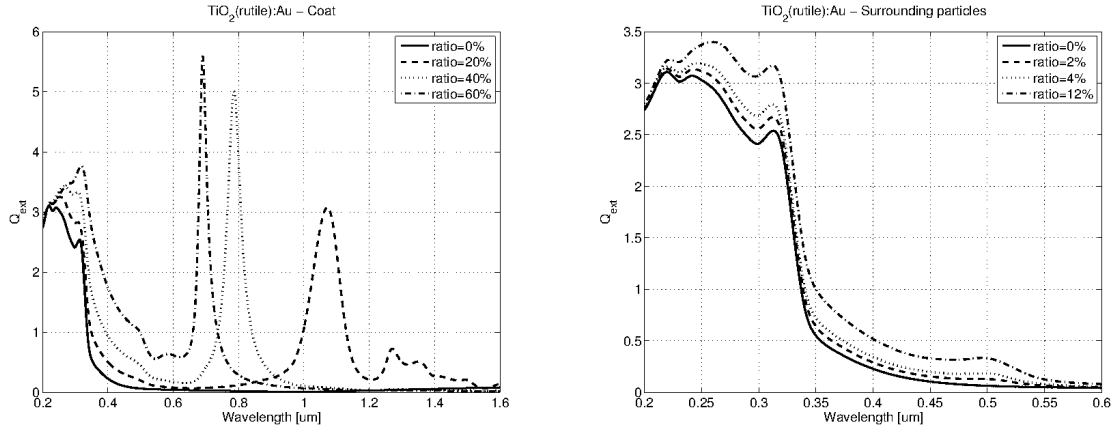

Figure 9: Extinction efficiency Q_{ext} as a function of the incident wavelength λ for $TiO_2(rutile) : Au$ composites.

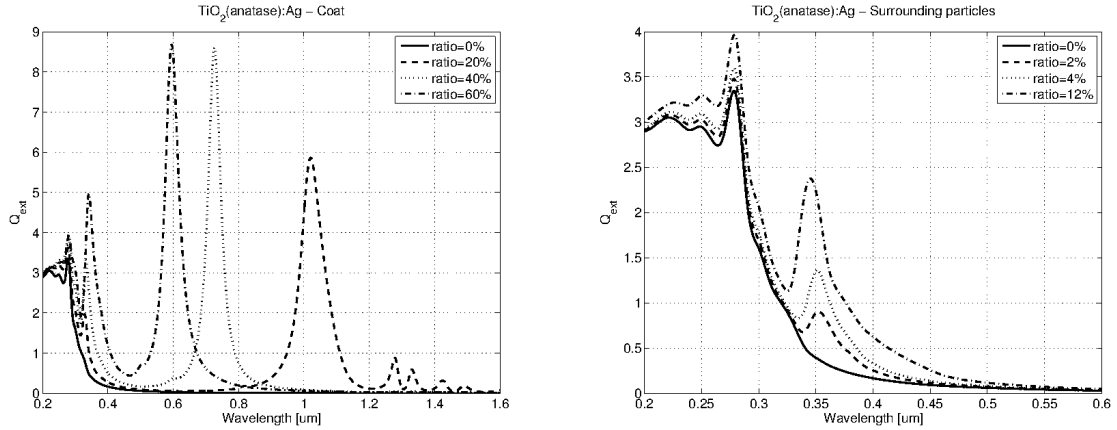

Figure 10: Extinction efficiency Q_{ext} as a function of the wavelength λ for $TiO_2(anatase) : Ag$ composites. Surrounding Ag particles are responsible for the extinction peak that occurs at the wavelength of ca. $\lambda \approx 350nm$.

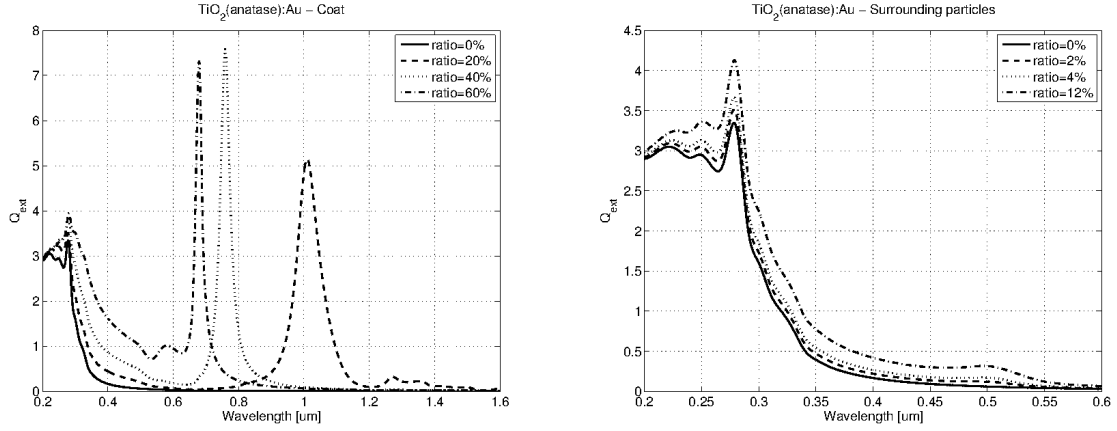

Figure 11: Extinction efficiency Q_{ext} as a function of the wavelength λ for $TiO_2(anatase) : Au$ composites.

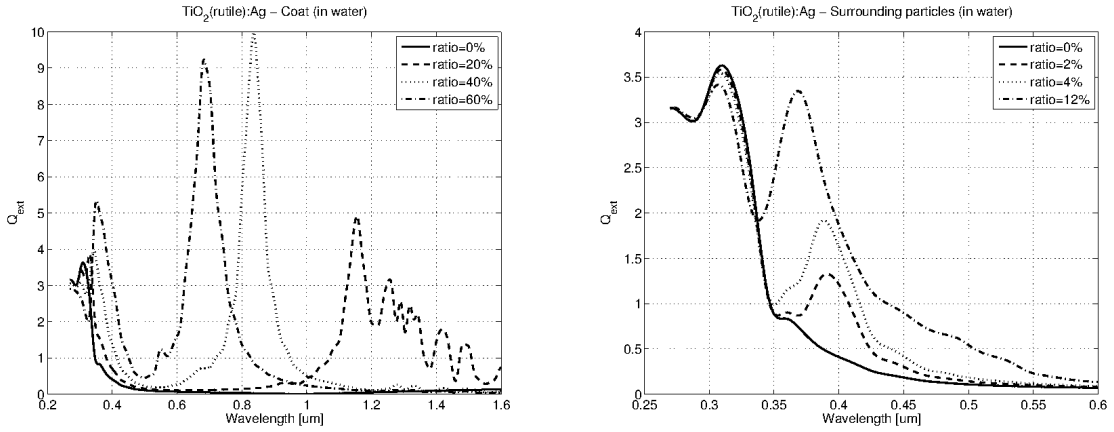

Figure 12: Extinction efficiency Q_{ext} as a function of the wavelength λ for $TiO_2(rutile) : Au$ composites immersed in water.

Its magnitude depends on the number of surrounding Ag spheres. No spectral effects were observed at the wavelength of $\lambda = 600nm$ and above. When coating is considered, the results are very different. Providing that the Ag layer is relatively small, e.g. $R_c - R_m = 1.3nm$, only minor aberrations occur in the non-visible spectrum from $\lambda = 1000nm$ to $\lambda = 2000nm$. By the contrary, when the volume of the external layer V_l is more significant, the second extinction peak appears and its position can be controlled by the thickness of the coat. Our study show that these two composite types cannot be used interchangeably because they lead to different results.

REFERENCES

[1] Landmann, M., Rauls, E., and Schmidt, W. G., "The electronic structure and optical response of rutile, anatase and brookite tio2," *Journal of Physics: Condensed Matter* **24**, doi:10.1088/0953–8984/24/19/195503 (2012).

[2] Hari, M., Joseph, S. A., Mathew, S., Radhakrishnan, P., and Nampoori, V. P. N., "Band-gap tuning and nonlinear optical characterization of ag:tio2 nanocomposites," *Journal of Applied Physics* **7**, http://dx.doi.org/10.1063/1.4757025 (2012).

[3] Nino-Martinez, N., Martinez-Castanon, G. A., Aragon-Pina, A., Martinez-Gutierrez, F., Martinez-Mendoza, J. R., and Ruiz, F., "Characterization of silver nanoparticles synthesized on titanium dioxide fine particles," *Nanotechnology* **19**, doi:10.1088/0957–4484/19/6/065711 (2008).

[4] Sunada, K., Watanabe, T., and Hashimoto, K., "Bactericidal activity of cooper-deposited tio2 thin film under weak uv light illumination," *Environmental Science and Technology* **37**, 4785–4789 (2003).

[5] Mroczka, J., "The cognitive process in metrology," *Measurement* **46**, 2896–2907 (2013).

[6] Palik, E., [*Handbook of Optical Constants of Solids*], Academic Press (1985).

[7] Polyanskiy, M., "Refractive info database, http://refractiveindex.info," (2013).

[8] Wozniak, M., Onofri, F. R. A., Barbosa, S., Yon, J., and Mroczka, J., "Comparison of methods to derive morphological parameters of multi-fractal samples of particle aggregates from tem images," *Journal of Colloid and Interface Science* **47**, 12–26 (2012).

[9] Mroczka, J., Wozniak, M., and Onofri, F. R. A., "Algorithms and methods for analysis of the optical structure factor of fractal aggregates," *Metrology and Measurements Systems* **19**, 459–470 (2012).

[10] Mroczka, J., "Method of moments in light scattering data inversion in the particle size distribution function," *Optics Communications* **99**, 147–151 (1993).

[11] Mroczka, J. and Wysoczanski, D., "Light scattering maps analysis to determine particles placement and concentration," *Proceedings of SPIE - The International Society for Optical Engineering* **10.1117/12.662237** (2006).

[12] Skorupski, K., Mroczka, J., Riefler, N., Oltmann, H., Will, S., and Wriedt, T., "Effect of the necking phenomenon on the optical properties of soot particles," *Journal of Quantitative Spectroscopy and Radiative Transfer* **10.1016/j.jqsrt.2014.03.001** (2014).

[13] Xu, Y. and Gustafson, B., "A generalized multiparticle mie-solution: further experimental verification," *Journal of Quantitative Spectroscopy and Radiative Transfer* **15**, 395–419 (2001).

[14] Mackowski, D. and Mischenko, M., "A multiple sphere t-matrix fortran code for use on parallel computer clusters," *Journal of Quantitative Spectroscopy and Radiative Transfer* **112**, 2182–2192 (2011).